Methane Oxidation

International Edition: DOI: 10.1002/anie.201604708
German Edition: DOI: 10.1002/ange.201604708

Low-Temperature Transformation of Methane to Methanol on Pd_1O_4 Single Sites Anchored on the Internal Surface of Microporous Silicate

*Weixin Huang, Shiran Zhang, Yu Tang, Yuting Li, Luan Nguyen, Yuanyuan Li, Junjun Shan, Dequan Xiao, Raphael Gagne, Anatoly I. Frenkel, and Franklin (Feng) Tao**

Abstract: *Direct conversion of methane to chemical feedstocks such as methanol under mild conditions is a challenging but ideal solution for utilization of methane. Pd_1O_4 single-sites anchored on the internal surface of micropores of a microporous silicate exhibit high selectivity and activity in transforming CH_4 to CH_3OH at 50–95 °C in aqueous phase through partial oxidation of CH_4 with H_2O_2. The selectivity for methanol production remains at 86.4 %, while the activity for methanol production at 95 °C is about 2.78 molecules per Pd_1O_4 site per second when 2.0 wt % CuO is used as a co-catalyst with the Pd_1O_4@ZSM-5. Thermodynamic calculations suggest that the reaction toward methanol production is highly favorable compared to formation of a byproduct, methyl peroxide.*

Methane is a relatively inexpensive resource.[1] Hydraulic fracturing supplies much of this earth-abundant source from shale, which make chemical and energy transformations economical.[2] One application of methane is the production of methanol. Currently, chemical industries use a two-step process in methanol production from methane, including steam reforming to generate synthetic gas (CO and H_2) and a following synthesis of methanol from CO and H_2. The first step is performed at a high temperature of 600–800 °C. The durability of catalysts at such a high temperature is quite low. In addition, a significant amount of energy is needed to perform the catalysis at such a high temperature. An ideal approach for utilization of CH_4 is a direct conversion of CH_4 to CH_3OH under mild conditions at a relatively low temperature because this transformation is thermodynamically feasible even at low temperature. Unfortunately, realization of this approach has remained challenging.

It has been reported that Cu-, Fe-, or Ni-exchanged ZSM-5 can form unique oxide species, including a bent mono(μ-oxo)di-metal structure upon activation with O_2 or N_2O[3] at a high temperature; the oxygen atoms in this bent mono(μ-oxo)di-metal structure oxidize methane to methanol at a temperature higher than 200 °C in the gas phase. Unfortunately, once these uniquely anchored oxygen species are consumed by CH_4, they have to be regenerated through an oxidation step of O_2 or N_2O at a high temperature. The regeneration can be done only after CH_3OH is removed from the internal surface of those micropores. The removal is typically done by soaking the used catalyst in a solvent and then dissolving methanol molecules in the solvent. Thus, the transformation of CH_4 to methanol by these unique oxide species anchored in ZSM-5 at high temperatures in the gas phase is mainly an oxidation reaction instead of a continuous catalytic process.[3c]

In contrast to the above chemical transformation of CH_4 to CH_3OH at a solid–gas interface in ZSM-5, metal cations of Fe, Cu, and Ni encapsulated in ZSM-5, and even commercial ZSM-5 alone,[4] are active in the direct oxidation of CH_4 to formic acid or even CH_3OH at a solid–liquid interface when H_2O_2 is used as an oxidant. The conversion rate of CH_4 to CH_3OH at a solid–liquid interface pioneered by Hutchings et al.[4a,5] is typically higher than these at a solid–gas interface,[3a,b] though the rate is still relatively low.

Although catalytic activity for direct oxidation of CH_4 to CH_3OH on these catalysts at solid–gas and solid–liquid interfaces was reported,[1,3–6] challenges remain before a direct oxidation process under mild conditions could be considered as a potential approach in the chemical industry. One challenge is that the activity and selectivity for production of methanol from CH_4 are far below the requirement of industrial production; another is the lack of fundamental understanding of the catalytic mechanism performed at a solid–liquid interface. To address these challenges, development of new catalysts with higher activity and selectivity under mild conditions, together with a fundamental understanding of the catalytic mechanism, is necessary. Herein, a catalyst consisting of Pd_1O_4 single-sites anchored on the internal surface of micropores of ZSM-5 was synthesized. Its performance in the catalytic transformation of CH_4 at a solid/liquid/gas interface was explored. Thermodynamic calculations for the formation of methanol or methyl preoxide were performed to understand the transformation of CH_4 to methanol from a thermodynamics point of view.

[*] W. Huang, Dr. S. Zhang, Y. Tang, Y. Li, Dr. L. Nguyen, Dr. J. Shan, Prof. Dr. F. Tao
Department of Chemical and Petroleum Engineering and Department of Chemistry, University of Kansas
Lawrence, KS 66045 (USA)
E-mail: franklin.feng.tao@ku.edu
Dr. Y. Li
Department of Physics, Yeshiva University
New York, NY 10016 (USA)
Prof. Dr. D. Xiao, R. Gagne
Department of Chemistry and Chemical Engineering
University of New Haven
West Haven, CT 06516 (USA)
Prof. Dr. A. I. Frenkel
Department of Materials Science and Chemical Engineering
Stony Brook University
Stony Brook, NY 11794 (USA)

Supporting information for this article can be found under: http://dx.doi.org/10.1002/anie.201604708.

Singly dispersed precious metal atoms anchored on oxides could offer a distinctly different electronic state in contrast to continuously packed metal atoms on the surface of a metal nanoparticle, and thus could exhibit a distinctly different catalytic activity or/and selectivity.[2b,7] Herein, we prepared catalysts with singly dispersed Pd_1O_4 sites anchored on the internal surface of micropores of ZSM-5. As described in the experimental section, the amount of loaded Pd cations is important for the preparation of singly dispersed Pd_1O_4 sites in ZSM-5. TEM images (Figure S1 a), the Pd 3d XPS spectrum (red line in Figure S2), and the XRD pattern (Figure S3) suggest that there are no PdO nanoparticles formed on ZSM-5 of 0.01 wt % Pd/ZSM-5. This suggests that the Pd atoms of 0.01 wt % Pd-ZSM-5 are singly dispersed on the internal surface of the micropores of ZSM-5. However, PdO nanoparticles were formed on 2.0 wt % Pd/ZSM-5 (Figures S1b, S2, and S3).

Pd K-edge Extended X-ray Absorption Fine Structure (EXAFS) experiments were performed to identify the coordination environment of Pd atoms anchored in ZSM-5. Unfortunately, owing to the low signal/noise ratio of the Pd K edge absorption spectra of 0.01 wt % Pd/ZSM-5, no conclusive information was acquired. A reasonable signal/noise ratio was obtained on 0.04 wt % Pd/ZSM-5. XPS studies of 0.04 wt % Pd/ZSM-5 (Figure S2) showed that no PdO nanoparticles were formed for 0.04 wt % Pd/ZSM-5. This suggests that the Pd atoms could be singly dispersed. Figure 1 presents Fourier transform magnitudes of k^2-weighted EXAFS data of 0.04 wt % Pd/ZSM-5 (blue line), pure Pd foil (black), and pure PdO nanoparticles (red). The Pd atoms in 0.04 wt % Pd/ZSM-5 exhibited a coordination environment distinctly different from metal Pd foil and PdO nanoparticles. In metallic Pd foil, the main peak at 2.58 Å is assigned to Pd–Pd bonds. There is no such peak in this r-range in the spectrum of 0.04 wt % Pd/ZSM-5 (blue line), showing no evidence for formation of metallic Pd nanoparticles on the catalyst, 0.04 wt % Pd/ZSM-5.

The average coordination number of O atoms to a Pd atom of 0.04 wt % Pd/ZSM-5 is 4.12 ± 0.49 (Table 1). In both the reported *r*-space EXAFS spectra of PdO nanoparticles[6a] and our studies of reference PdO sample, a peak at 3.1 Å was clearly identified, comparable in intensity to be the first

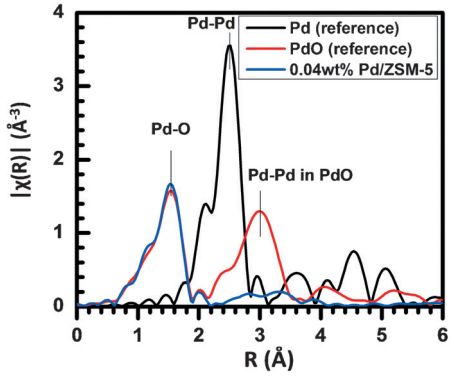

Figure 1. Fourier transform magnitudes of k^2-weighted EXAFS data of 0.04 wt % Pd/ZSM-5 (blue) and reference samples, including Pd foil (red) and PdO nanoparticles (black).

Table 1: Coordination number of O or Pd atoms to a Pd atom, and bond lengths of O–Pd or Pd–Pd in 0.04 wt %Pd/ZSM-5 studied with EXAFS.

Sample	N (Pd–Pd)	N (Pd–O)	R(Pd–Pd) [Å]	R (Pd–O) [Å]
Pd foil	12	0	2.740 ± 0.002	–
0.04 wt % Pd/ZSM-5	0	4.12 ± 0.49	–	2.001 ± 0.009

nearest neighbor Pd–O contribution; this peak at 3.1 Å represents the contribution to EXAFS from the two closest Pd atoms in a PdO nanoparticle, bridged by an oxygen atom (Pd–O–Pd). Compared to other PdO nanoparticles[6a] and the reference PdO sample (red line in Figure 1), however, the *r*-space spectrum of 0.04 wt % Pd/ZSM-5 (blue line in Figure 1) does not have such a distinct peak with the similar intensity as the Pd–Pd peak in PdO at ~3.1 Å. Therefore, there is no evidence that any species or structure in 0.04 wt % Pd/ZSM-5 contains Pd–O–Pd species, which indicates the absence of PdO nanoclusters. In addition, the measured coordination number of oxygen atoms to a Pd atom, 4.12 ± 0.49 suggests the lack of the potential bent mono(μ-oxo)dipalladium structure since the coordination number of oxygen atoms around a Pd atom CN(Pd-O) in a mono(μ-oxo)dipalladium (Figure S4a) is expected to be 3 instead of 4.[3c,4a] Based on 1) the lack of a Pd–Pd bond, 2) the lack of a Pd–O–Pd bond, and 3) the measured coordination number of oxygen atoms coordinating to a Pd atom, we conclude that the Pd atoms in 0.04 wt % Pd/ZSM-5 exist as singly dispersed Pd_1O_4 species in ZSM-5 (Figure S4 b).

Temperature-dependent catalytic performances of Pd/ZSM-5 were measured in the range of 50–95 °C which is lower than the boiling point of H_2O_2 at a high pressure of 30 bar of CH_4 (Table S1). As shown in Table S1, the yield of total products is highly dependent upon the temperature. For example, the total yield is about 399.4 μmol (about 0.40 mmol) produced from 0.01 wt % Pd/ZSM-5 (28 mg catalyst) at 95 °C within 30 minutes (entry 5 of Table S1), which is about 3 times larger than the same catalyst at 50 °C (entry 1 of Table S1). The amounts of each product formed at 50, 70, and 95 °C are listed in Table S1.

Figure S5 presents the products formed from methane partial oxidation on 0.01 wt % Pd/ZSM-5 at 50 °C, which are mainly formic acid, methyl peroxide, methanol, and carbon dioxide with yields of 60.82, 39.48, 7.39, and 4.22 μmol, respectively, with a total yield of 111.91 μmol. Blank experiment of pure H-ZSM-5 at 50 °C (pink bars in Figure S5) showed that the activity for oxidation of CH_4 with H_2O_2 by pure H-ZSM-5 was lower than 0.01 wt % Pd/ZSM-5 under the same conditions at 50 °C. In addition, the total yields of these products on 28 mg of 0.01 wt % Pd supported on Al_2O_3 nanoparticles and 28 mg of 0.01 wt % Pd supported on SiO_2 nanoparticles at 50 °C are only a few μmol, respectively (Figure S5). These studies suggested that Pd cations anchored on open surfaces (surface of Al_2O_3 or SiO_2 nanoparticles) are not active for this transformation at 50 °C.

With the same synthesis steps as 0.01 wt % Pd/ZSM-5, catalysts of ZSM-5 loaded with different amounts of Pd

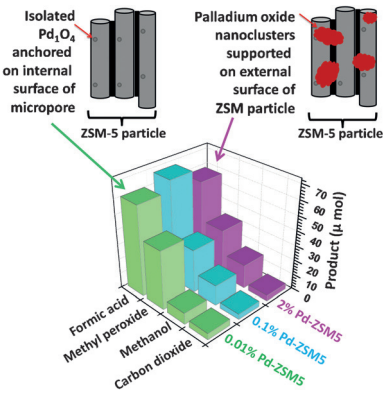

Figure 2. Yields of products of transformation of CH_4 catalyzed by 0.01, 0.10, and 2.0 wt% Pd/ZSM-5 for methane partial oxidation at 50 °C.

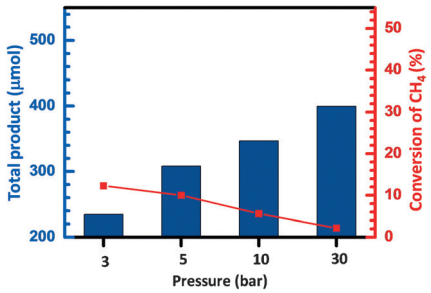

Figure 3. Pressure-dependent catalytic performance in partial oxidation of CH_4 on 0.01 wt% Pd/ZSM-5 at 95 °C. 28 mg of catalyst, 0.01 wt% Pd/ZSM-5 was added to a Parr reactor; 10 mL de-ionized H_2O was added; H_2O_2 (5 mmol) was added to H_2O before CH_4 was introduced to the Parr reactor. The plotted yield of a product formed on 28 mg 0.01 wt%Pd/ZSM-5 is the value after subtraction of the yield of the products formed on 28 mg ZSM-5 (without Pd sites) under the same catalytic conditions.

precursors were synthesized. Figure 2 presents the yields of the four main products including formic acid, methyl peroxide, methanol, and CO_2 catalyzed by 0.01, 0.02, 0.10, and 2.0 wt% Pd/ZSM-5 at 50 °C. Interestingly, these catalysts exhibit quite similar yields of the four products, although their loadings of Pd precursor were very different. The similarity in catalytic performances on ZSM-5 with quite different loadings suggests that the extra Pd atoms likely remain on the external surface of ZSM-5 particles and do not play any role in the generation of these products. TEM image (Figure S1 b), XPS (Figure S2), and XRD (Figure S3) clearly showed the formation of a large number of small PdO nanoparticles on the external surface of ZSM-5 particles when the loading of Pd precursor was 2.0 wt%. Because the yield of the four products from 2.0 wt% Pd/ZSM-5 was similar or even lower than 0.01 wt% Pd/ZSM-5 (Figure 2), we can deduce that the PdO nanoparticles are not active in these chemical transformations.

Methane-pressure-dependent catalytic performances including conversion of CH_4 (red segment line in Figure 3) and amount of total products (blue bars in Figure 3) formed on the same catalyst 28 mg of 0.01 wt% Pd/ZSM-5 at 95 °C were studied. As shown in Figure 3, the total yield is about 234 μmol and the conversion is about 12.3% when the CH_4 pressure was 3 bar. This shows that the partial oxidation of methane can be performed on 0.01 wt% Pd/ZSM-5 even at a low pressure of CH_4.

As shown in Figure 4 a, the molecular fraction of methanol among the total product (formic acid, methyl peroxide, methanol, and CO_2) on 0.01 wt% Pd/ZSM-5 is quite low, with formic acid being the major product. As methanol could be oxidized to formic acid by H_2O_2 under mild conditions, the observed formic acid in Figure 4 a could be formed from further oxidation of methanol by H_2O_2 after methanol was produced on 0.01 wt% Pd/ZSM-5. In fact, our control experiments confirmed that the formed methanol can be readily oxidized to formic acid by H_2O_2 (see Section 5 of the Supporting Information).

Based on the conversion of CH_4 (Figure 3), the amount of the introduced H_2O_2 is more than the oxidant needed for formation of these detected products. Thus, there was extra

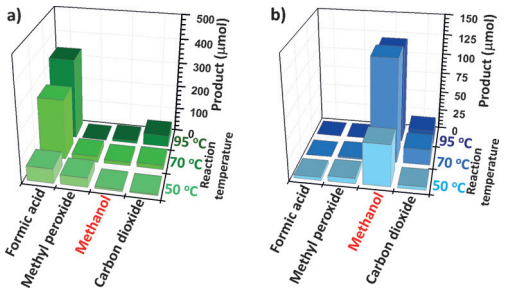

Figure 4. Catalytic performance of a) 0.01 wt% Pd/ZSM-5 at 50, 70, and 95 °C, and b) 0.01 wt% Pd/ZSM-5 loaded with 2 wt% CuO at 50, 70, and 95 °C. The plotted yields of products formed on 28 mg 0.01 wt%Pd/ZSM-5 or 0.01 wt%Pd/ZSM-5 loaded with 2.0 wt%CuO are the values after subtraction of the yields of the products formed on 28 mg ZSM-5 (without Pd sites) under the same catalytic conditions.

H_2O_2 after the formation of methanol. Unfortunately, the extra H_2O_2 oxidized the methanol to formic acid (see Section 5 of the Supporting Information). The facile oxidation of methanol to formic acid at 95 °C by H_2O_2 in fact largely decreased the concentration of initially formed methanol and thus significantly increased the concentration of formic acid. Thus, removal of the extra H_2O_2 could prevent methanol from being oxidized to formic acid by H_2O_2 and could promote the selectivity for production of methanol. Here, CuO was used to catalyze the dissociation of H_2O_2 to H_2O and O_2. We confirmed that the decomposition of H_2O_2 to H_2O and O_2 can be catalyzed by CuO (Section 6 in the Supporting Information). Next, 2.0 wt% CuO was impregnated in 0.01 wt% Pd/ZSM-5 as a co-catalyst for dissociating extra H_2O_2 after formation of methanol.

Compared to 0.01 wt% Pd/ZSM-5 without CuO (entries 1, 3, and 5 of Table S1), the selectivities for production of methanol on 0.01 wt% Pd/ZSM-5 loaded with 2 wt% CuO at 50, 70, and 95 °C (entries 2, 4, and 6 of Table S1) were 78.48, 85.46, and 86.35%, respectively, indicating that the CuO co-catalyst significantly increased the selectivity for

methanol production. The preservation of selectivity in 78–86% in the temperature range of 50–95 °C suggests that 78–86% is the selectivity for production of CH_3OH from CH_4 on Pd_1O_4 sites.

Turn-over frequency (TOF) is used as a scale to evaluate catalytic activity, although it is challenging to accurately measure the number of active sites Pd_1O_4 anchored in ZSM-5. The details of the calculations of TOFs were described in Section 8 of the Supporting Information. Table 2 lists the evaluated TOFs of 0.01 wt% Pd/ZSM-5 at different temperatures with (or without) the CuO co-catalyst. TOFs of producing CH_3OH from CH_4 on reported catalysts, including 2.5 wt% Fe/ZSM-5 and Au-Pd/TiO_2, were evaluated for comparison[4a,5] (see Sections 8.2 and 8.3 of the Supporting Information). The TOFs for producing organic compounds (methanol, formic acid, and methane peroxide) catalyzed by 0.01 wt% Pd/ZSM-5 without CuO at 50, 70, and 95 °C were 2.45, 6.68, and 8.30 molecules on a Pd_1O_4 site per second, respectively (entries 1–3 in Table 2). Formic acid was the major product. The TOFs of the CH_3OH produced on 0.01 wt% Pd/ZSM-5 with loaded 2.0 wt% CuO at 50, 70, and 95 °C (entries 4–6 in Table 2) are 1.53–2.33 CH_3OH molecules per site per second, were higher than those of reported catalysts at solid–liquid interfaces[4a,5] (see Section 8.1 of the Supporting Information). These TOFs of this work were obtained by using the amounts of products generated on Pd_1O_4 sites after subtracting the products formed on the substrate (ZSM-5) under the corresponding catalytic conditions.

Table 2: TOFs for methane partial oxidation on 0.01 wt% Pd/ZSM-5 and other catalysts that convert CH_4 to CH_3OH and other organic oxygenates at solid–liquid interfaces.

Entry	Catalyst	Temp. [°C]	TOF[a] all products[c]	TOF[b] methanol only[c]
1	0.01 wt%Pd/ZSM-5	50	2.45	N.A. [d]
2	0.01 wt% Pd/ZSM-5	70	6.68	N.A.[d]
3	0.01 wt% Pd/ZSM-5	95	8.30	N.A. [d]
4	0.01 wt% Pd/ZSM-5 +2 wt% CuO	50	1.46	1.53
5	0.01 wt% Pd/ZSM-5 +2 wt% CuO	70	3.19	2.72
6	0.01 wt% Pd/ZSM-5 +2 wt% CuO	95	2.78	2.33

[a] TOF $= \frac{\text{moles of all organic prodcuts}}{\text{moles of metal} \times \text{time (in second)}}$. [b] TOF $= \frac{\text{moles of methanol}}{\text{moles of metal} \times \text{time (in second)}}$. [c] The number of Pd_1O_4 active sites is 1.58×10^{16}. [d] As the amount of the produced methanol is up to 13 μmol (see Table S1), the error bars of the TOFs of these catalysts are large. [e] The detailed calculations of the TOFs and comparison with other reported values is discussed in Section 8 of the Supporting Information.

As the size of ZSM-5 particles used in this work are in the range of 100–300 nm, the length of the micropores in these ZSM-5 particles is in the scale range of ZSM-5 particles. In the liquid phase, the diffusion of Pd cations to deep parts of these micropores is limited. Both the diffusion of CH_4 from the aqueous phase to Pd_1O_4 sites anchored on the internal surface of microspores and the diffusion of product molecules from catalytic sites in micropores to the aqueous phase are limited by the long micropores to some extent. These limits are closely relevant to the limited conversion of CH_4 here.

To understand the high activity and selectivity for the production of CH_3OH on Pd_1O_4 of 0.01 wt% Pd/ZSM-5, DFT calculations of thermodynamics of the formation of methanol and methyl peroxide were performed as described in Section 9 of the Supporting Information. Based on our calculations, the formation of methanol is thermodynamically favorable over methyl peroxide. This is consistent with the higher catalytic selectivity for methanol compared to methyl peroxide (entries 2, 4 and 6 of Table S1).

Acknowledgements

This work was supported by KU research fund, Chemical Sciences, Geosciences and Biosciences Division, Office of Basic Energy Sciences, Office of Science, U.S. Department of Energy, under Grant No. DE-SC0014561. The EXAFS studies were supported by DE-FG02-03ER15476 (to AIF). Beamline X18B of the NSLS was supported in part by Synchrotron Catalysis Consortium under the U.S. DOE Grant No. DE-SC0012335.

Keywords: methane · methanol · oxidation · palladium · single-sites

How to cite: *Angew. Chem. Int. Ed.* **2016**, *55*, 13441–13445
Angew. Chem. **2016**, *128*, 13639–13643

[1] S. R. Golisz, T. B. Gunnoe, W. A. Goddard, J. T. Groves, R. A. Periana, *Catal. Lett.* **2011**, *141*, 213–221.
[2] a) Exxonmobil, **2013**, http://corporate.exxonmobil.com/en/energy/energy-outlook; b) X. Guo, G. Fang, G. Li, H. Ma, H. Fan, L. Yu, C. Ma, X. Wu, D. Deng, M. Wei, D. Tan, R. Si, S. Zhang, J. Li, L. Sun, Z. Tang, X. Pan, X. Bao, *Science* **2014**, *344*, 616–619.
[3] a) E. V. Starokon, M. V. Parfenov, L. V. Pirutko, S. I. Abornev, G. I. Panov, *J. Phys. Chem. C* **2011**, *115*, 2155–2161; b) M. H. Groothaert, P. J. Smeets, B. F. Sels, P. A. Jacobs, R. A. Schoonheydt, *J. Am. Chem. Soc.* **2005**, *127*, 1394–1395; c) J. Shan, W. Huang, N. Luan, Y. Yu, S. Zhang, Y. Li, A. I. Frenkel, F. Tao, *Langmuir* **2014**, *30*, 8558–8569.
[4] a) C. Hammond, M. M. Forde, M. H. Ab Rahim, A. Thetford, Q. He, R. L. Jenkins, N. Dimitratos, J. A. Lopez-Sanchez, N. F. Dummer, D. M. Murphy, A. F. Carley, S. H. Taylor, D. J. Willock, E. E. Stangland, J. Kang, H. Hagen, C. J. Kiely, G. J. Hutchings, *Angew. Chem. Int. Ed.* **2012**, *51*, 5129–5133; *Angew. Chem.* **2012**, *124*, 5219–5223; b) T. Sheppard, C. D. Hamill, A. Goguet, D. W. Rooney, J. M. Thompson, *Chem. Commun.* **2014**, *50*, 11053–11055; c) M.-L. Tsai, R. G. Hadt, P. Vanelderen, B. F. Sels, R. A. Schoonheydt, E. I. Solomon, *J. Am. Chem. Soc.* **2014**, *136*, 3522–3529; d) C. Hammond, N. Dimitratos, R. L. Jenkins, J. A. Lopez-Sanchez, S. A. Kondrat, M. H. Ab Rahim, M. M. Forde, A. Thetford, S. H. Taylor, H. Hagen, E. E. Stangland, J. H. Kang, J. M. Moulijn, D. J. Willock, G. J. Hutchings, *ACS Catal.* **2013**, *3*, 689–699; e) E. V. Starokon, M. V. Parfenov, S. S. Arzumanov, L. V. Pirutko, A. G. Stepanov, G. I. Panov, *J. Catal.* **2013**, *300*, 47–54.
[5] M. H. Ab Rahim, M. M. Forde, R. L. Jenkins, C. Hammond, Q. He, N. Dimitratos, J. A. Lopez-Sanchez, A. F. Carley, S. H. Taylor, D. J. Willock, D. M. Murphy, C. J. Kiely, G. J. Hutchings, *Angew.*

Chem. Int. Ed. **2013**, *52*, 1280 – 1284; *Angew. Chem.* **2013**, *125*, 1318 – 1322.

[6] a) K. Takao, K. Suzuki, T. Ichijo, S. Sato, H. Asakura, K. Teramura, K. Kato, T. Ohba, T. Morita, M. Fujita, *Angew. Chem. Int. Ed.* **2012**, *51*, 5893 – 5896; *Angew. Chem.* **2012**, *124*, 5995 – 5998; b) S. Grundner, W. Luo, M. Sanchez-Sanchez, J. A. Lercher, *Chem. Commun.* **2016**, *52*, 2553 – 2556; c) M. V. Parfenov, E. V. Starokon, L. V. Pirutko, G. I. Panov, *J. Catal.* **2014**, *318*, 14 – 21; d) P. J. Smeets, R. G. Hadt, J. S. Woertink, P. Vanelderen, R. A. Schoonheydt, B. F. Sels, E. I. Solomon, *J. Am. Chem. Soc.* **2010**, *132*, 14736 – 14738; e) N. V. Beznis, B. M. Weckhuysen, J. H. Bitter, *Catal. Lett.* **2010**, *138*, 14 – 22.

[7] a) S. Zhang, L. Nguyen, J.-X. Liang, J. Shan, J. Liu, A. I. Frenkel, A. Patlolla, W. Huang, J. Li, F. Tao, *Nat. Commun.* **2015**, *6*, 7938; b) F. F. Tao, J. J. Shan, L. Nguyen, Z. Y. Wang, S. R. Zhang, L. Zhang, Z. L. Wu, W. X. Huang, S. B. Zeng, P. Hu, *Nat. Commun.* **2015**, *6*, 7798; c) L. Nguyen, S. R. Zhang, L. Wang, Y. Y. Li, H. Yoshida, A. Patlolla, S. Takeda, A. I. Frenkel, F. Tao, *ACS Catal.* **2016**, *6*, 840 – 850; d) L. Wang, S. R. Zhang, Y. Zhu, A. Patlolla, J. J. Shan, H. Yoshida, S. Takeda, A. I. Frenkel, F. Tao, *ACS Catal.* **2013**, *3*, 1011 – 1019.

Received: June 9, 2016
Revised: August 21, 2016
Published online: September 26, 2016

